Supporting Information

Ruthenium-Caged Antisense Morpholinos for Regulating Gene Expression in Zebrafish Embryos

J.C. Griepenburg,[a] T.L. Rapp,[a] P.J. Carroll,[a] J. Eberwine,[b] and I.J. Dmochowski[a]

[a] Department of Chemistry, University of Pennsylvania, 231 South 34th Street, Philadelphia, Pennsylvania 19104, United States
[b] Department of Pharmacology, Perelman School of Medicine, University of Pennsylvania, 37 John Morgan Building, 3620 Hamilton Walk, Philadelphia, Pennsylvania 19104, United States

Table of Contents

Methods S1. Synthesis of $[Ru(bpy)_2(3\text{-ethynylpyridine})_2](Cl)_2$ (RuBEP)

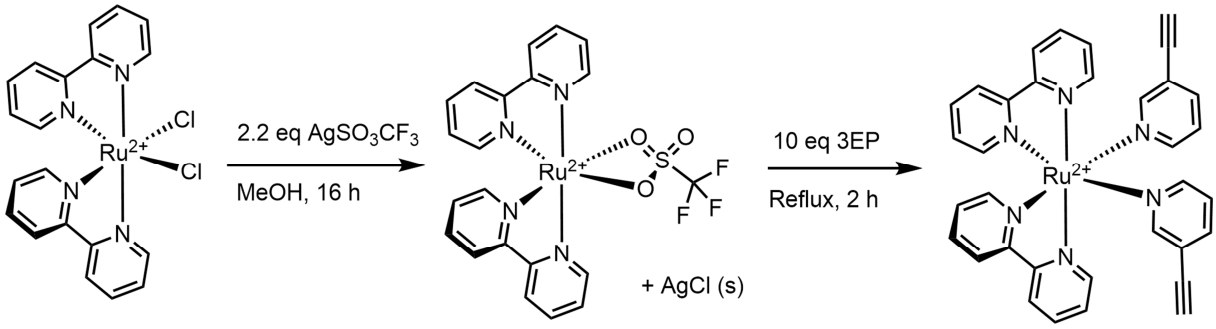

$Ru(bpy)_2Cl_2$ (101.8 mg, 0.20 mmol) and $AgSO_3CF_3$ (105 mg, 0.41 mmol) were suspended in distilled methanol (10 mL). Solution was placed in the freezer overnight under nitrogen. The solution was then brought to rt, filtered to remove AgCl, and 3-ethynylpyridine (3EP, 201.7 mg, 0.40 mmol) was added. The reaction was heated to 75 ^oC for 5 h until no further changes were observed by UV-Vis spectroscopy. The methanol was removed under reduced pressure and product was redissolved in boiling water. Solid ammonium hexafluorophosphate was added to the chilled solution until a light orange precipitate was formed. This was vacuum filtered, washed twice with cold water and dried. Compound was further purified by 1.5 x 15 cm silica column (230-400 mesh) with 9:1 dichloromethane:acetonitrile as eluent and isolated in 71% yield (106.6 mg, 0.12 mmol). The water-soluble chloride salt was synthesized by addition of tetrabutylammonium chloride to a solution of $[Ru(bpy)_2(3EP)_2](PF_6)_2$ dissolved in acetone.

^{1}H NMR (500 MHz, CD_3CN) 3.74 (s, 1H, 3EP-H_5), 7.33 (dd, 1H, J = 7.9, 3EP-H_3), 7.39 (ddd, 1H, J = 6.7, bpy-H_3), 7.82 (ddd, 1H, J = 6.4, bpy-H_6), 7.90 (d, 1H, J = 5.4, bpy-H_1), 7.95 (dd, 1H, J = 5.8, 3EP-H_2), 7.97 (dd, 1H, J = 7.6, bpy-H_2), 8.19 (td, 1H, J = 7.9, bpy-H_7), 8.31 (d, 1H, J = 8.2, bpy-H_4), 8.32 (d, 1H, J = 5.2, 3EP-H_1), 8.38 (s, 1H, 3EP-H_4), 8.40 (d, 1H, J = 7.9, bpy-H_5), 8.95 (d, 1H, J = 5.2, bpy-H_8).

^{13}C NMR (500 MHz, CD_3CN) 78.8, 84.5, 122.8, 124.9, 125.2, 126.9, 128.7, 129.0, 138.9, 139.2, 142.1, 153.5, 153.7, 154.5, 156.5, 158.6, 158.7.

Anal. Calc. for $C_{34}H_{12}N_6RuP_2F_{12}$: C, 65.90; H, 4.23; N, 13.56. Found: C, 66.2; H, 4.30; N, 13.7. MS(ES): *m/2z* 310.06, expected: *m/2z* 310.06

Figure S1. UV-Vis spectroscopy monitoring RuBEP synthesis

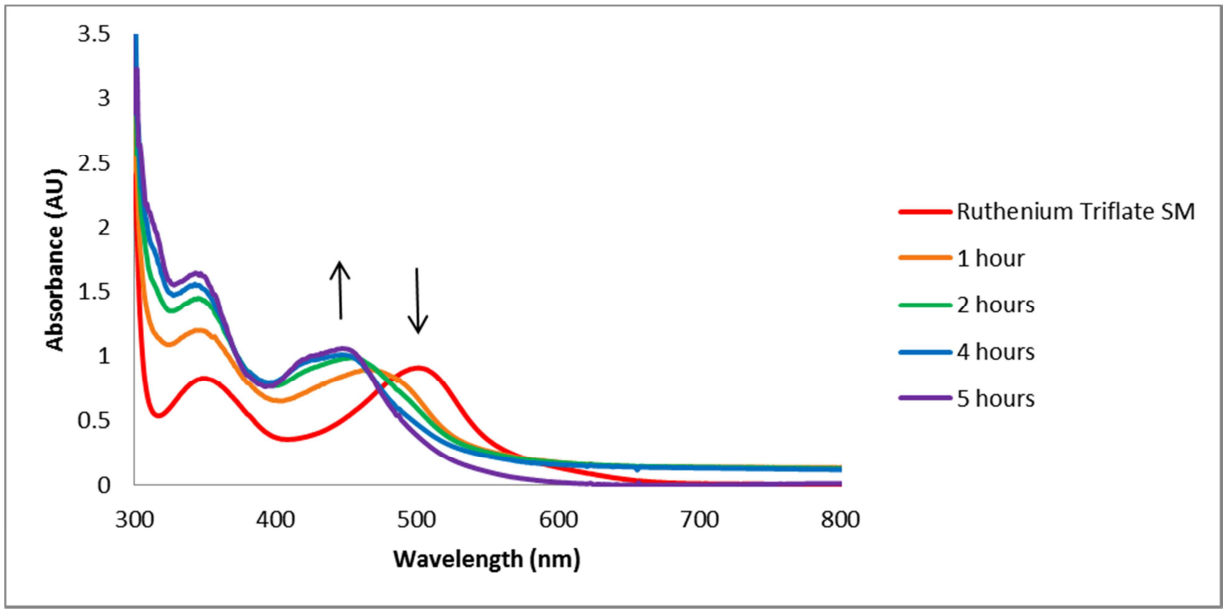

UV-Vis spectra of RuBEP synthesis (reaction solution was methanol, 75 ^{o}C). The peak at 520 nm was due to $Rubpy_2OTf$, which disappeared as RuBEP was formed to give the double peak near 450 nm.

Methods S2. Crystal structure of [RuBEP](PF$_6$)$_2$

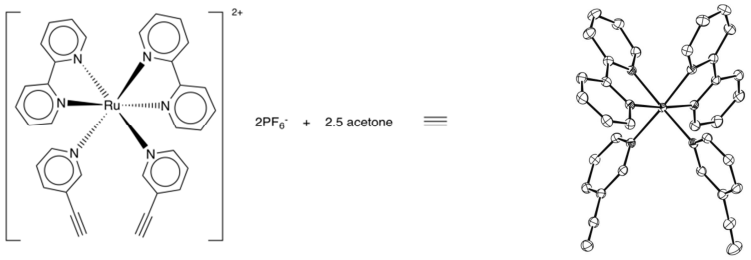

Compound $C_{34}H_{26}N_6P_2F_{12}Ru \cdot 2½$ acetone, crystallized in the Triclinic space group P$\bar{1}$ with a=11.2159(7)Å, b=12.5550(8)Å, c=18.1382(12)Å, α=70.206(3)°, β=85.323(3)°, γ=67.450(2)°, V=2216.1(2)Å^3, Z=2, and d_{calc} = 1.581 g/cm^3. X-ray intensity data were collected on a Bruker APEXII CCD area detector employing graphite-monochromated Mo-Kα radiation (λ=0.71073 Å) at a temperature of 100(1)K. Preliminary indexing was performed from a series of thirty-six 0.5° rotation frames with 10-sec exposures. A total of 2348 frames were collected with a crystal to detector distance of 37.6 mm, rotation widths of 0.5° and 20-sec exposures:

scan type	2Θ	ω	Φ	χ	frames
Φ	19.50	327.79	15.97	36.30	739
Φ	-20.50	342.55	321.55	-73.06	739
ω	-23.00	333.53	158.99	-70.01	64
ω	-15.50	340.80	341.11	-63.64	99
ω	-25.50	330.51	47.91	-56.95	185
ω	-25.50	239.19	209.98	28.88	204
ω	-18.00	243.20	310.97	36.30	208
ω	27.00	277.79	5.00	57.63	221
Φ	-10.50	318.39	249.35	52.47	254
ω	17.00	322.24	318.36	83.36	114
Φ	27.00	352.41	83.39	85.83	157
Φ	-18.00	124.02	292.98	-95.28	588

Rotation frames were integrated using SAINT,[a] producing a listing of unaveraged F^2 and σ(F^2) values which were then passed to the SHELXTL[b] program package for further processing

[a]Bruker (2009) SAINT. Bruker AXS Inc., Madison, Wisconsin, USA.

[b]Bruker (2009) SHELXTL. Bruker AXS Inc., Madison, Wisconsin, USA.

and structure solution. A total of 73021 reflections were measured over the ranges $1.86 \leq \theta \leq 27.54°$, $-14 \leq h \leq 14$, $-16 \leq k \leq 16$, $-23 \leq l \leq 23$ yielding 10200 unique reflections ($R_{int} = 0.0189$). The intensity data were corrected for Lorentz and polarization effects and for absorption using SADABS[c] (minimum and maximum transmission 0.6876, 0.7456).

The structure was solved by direct methods (SHELXS-97[d]). Refinement was by full-matrix least squares based on F^2 using SHELXL-97[1]. All reflections were used during refinement. The weighting scheme used was $w=1/[\sigma^2(F_o^2)+ (0.0907P)^2 + 0.3133P]$ where $P = (F_o^2 + 2F_c^2)/3$. Non-hydrogen atoms were refined anisotropically and hydrogen atoms were refined using a riding model. Refinement converged to R1=0.0266 and wR2=0.0630 for 9570 observed reflections for which $F > 4\sigma(F)$ and R1=0.0292 and wR2=0.0655 and GOF =1.051 for all 10200 unique, non-zero reflections and 643 variables.[e] The maximum λ/σ in the final cycle of least squares was 0.002 and the two most prominent peaks in the final difference Fourier were +1.120 and -0.826 e/Å^3.

Table S1 lists cell information, data collection parameters, and refinement data. Final positional and equivalent isotropic thermal parameters are given in Tables S2 and S3. Anisotropic thermal parameters are in Table S4. Tables S5 and S6 list bond distances and bond angles. Figure S2 is an ORTEP[f] representation of the molecule with 50% probability thermal ellipsoids displayed.

---

[c]Sheldrick, G.M. (2007) SADABS. University of Gottingen, Germany.

[e]$R1 = \Sigma||F_o| - |F_c|| / \Sigma |F_o|$

$wR2 = [\Sigma w(F_o^2 - F_c^2)^2/\Sigma w(F_o^2)^2]^{½}$

$GOF = [\Sigma w(F_o^2 - F_c^2)^2/(n - p)]^{½}$

where n = the number of reflections and p = the number of parameters refined.

[f]"ORTEP-II: A Fortran Thermal Ellipsoid Plot Program for Crystal Structure Illustrations". C.K. Johnson (1976) ORNL-5138.

Figure S2. ORTEP drawing of RuBEP with 50% probability thermal ellipsoids.

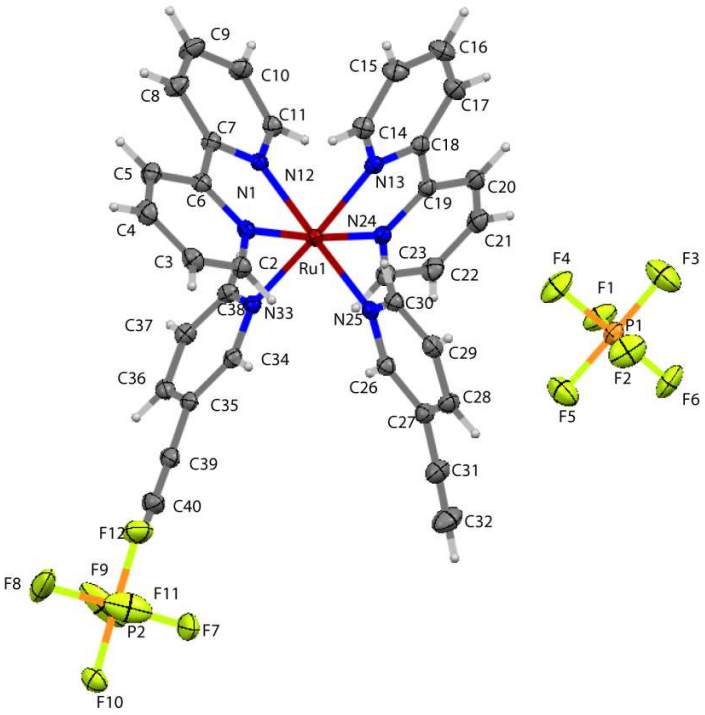

Table S1. Summary of Structure Determination of [RuBEP]$(PF_6)_2$

Empirical formula	$C_{83}H_{82}F_{24}N_{12}O_5P_4Ru_2$
Formula weight	2109.63
Temperature	100(1) K
Wavelength	0.71073 Å
Crystal system	Triclinic
Space group	$P\bar{1}$
Cell constants:	
a	11.2159(7) Å
b	12.5550(8) Å
c	18.1382(12) Å
α	70.206(3)°
β	85.323(3)°
γ	67.450(2)°
Volume	2216.1(2) $Å^3$
Z	1
Density (calculated)	1.581 Mg/m^3
Absorption coefficient	0.522 mm^{-1}
F(000)	1068
Crystal size	0.42 x 0.26 x 0.10 mm^3
Theta range for data collection	1.86 to 27.54°
Index ranges	$-14 \le h \le 14$, $-16 \le k \le 16$, $-23 \le l \le 23$

Reflections collected	73021
Independent reflections	10200 [R(int) = 0.0189]
Completeness to theta = 27.54°	99.6 %
Absorption correction	Semi-empirical from equivalents
Max. and min. transmission	0.7456 and 0.6876
Refinement method	Full-matrix least-squares on F^2
Data / restraints / parameters	10200 / 122 / 643
Goodness-of-fit on F^2	1.051
Final R indices [I>2sigma(I)]	R1 = 0.0266, wR2 = 0.0630
R indices (all data)	R1 = 0.0292, wR2 = 0.0655
Largest diff. peak and hole	1.120 and -0.826 e.$Å^{-3}$

Table S2. Refined Positional Parameters for [RuBEP]$(PF_6)_2$

Atom	x	y	z	U_{eq}, Å^2
Ru1	0.506258(11)	0.163868(11)	0.264396(7)	0.01291(4)
N1	0.65818(12)	0.13185(12)	0.19098(8)	0.0153(2)
N12	0.45450(12)	0.07306(12)	0.20479(8)	0.0149(2)
N13	0.57466(12)	-0.00632(12)	0.34959(8)	0.0155(2)
N24	0.35555(13)	0.17812(12)	0.33876(8)	0.0154(2)
N25	0.57819(13)	0.24338(12)	0.32652(8)	0.0155(2)
N33	0.41533(12)	0.33223(12)	0.17585(8)	0.0151(2)
C2	0.75831(15)	0.16753(15)	0.18526(10)	0.0188(3)
C3	0.85450(16)	0.14474(16)	0.13324(10)	0.0219(3)
C4	0.84615(17)	0.08520(16)	0.08327(10)	0.0235(3)
C5	0.74281(16)	0.04878(16)	0.08769(10)	0.0218(3)
C6	0.65119(15)	0.07173(14)	0.14269(9)	0.0169(3)
C7	0.54123(15)	0.03182(14)	0.15400(9)	0.0173(3)
C8	0.52811(17)	-0.04635(17)	0.11907(11)	0.0247(4)
C9	0.42495(18)	-0.08374(17)	0.13656(12)	0.0272(4)
C10	0.33660(17)	-0.04140(16)	0.18777(10)	0.0226(3)
C11	0.35404(15)	0.03707(15)	0.22011(9)	0.0180(3)
C14	0.68458(15)	-0.09937(15)	0.34717(10)	0.0195(3)
C15	0.71162(17)	-0.21890(16)	0.39519(11)	0.0247(4)
C16	0.62293(18)	-0.24480(16)	0.44906(11)	0.0261(4)
C17	0.51085(17)	-0.14999(16)	0.45341(10)	0.0222(3)
C18	0.48813(15)	-0.03161(14)	0.40305(9)	0.0165(3)
C19	0.36860(15)	0.07434(14)	0.40007(9)	0.0161(3)
C20	0.27411(16)	0.07009(16)	0.45418(10)	0.0204(3)
C21	0.16281(17)	0.17312(17)	0.44612(10)	0.0235(3)
C22	0.15004(17)	0.27882(16)	0.38419(11)	0.0239(3)
C23	0.24783(16)	0.27815(15)	0.33221(10)	0.0198(3)
C26	0.50882(15)	0.35333(14)	0.33424(9)	0.0173(3)
C27	0.55503(16)	0.40441(15)	0.37742(10)	0.0200(3)
C28	0.67825(17)	0.33911(15)	0.41461(10)	0.0211(3)
C29	0.75013(16)	0.22637(15)	0.40647(10)	0.0198(3)
C30	0.69787(15)	0.18182(14)	0.36276(9)	0.0172(3)
C31	0.47574(18)	0.52329(17)	0.38143(11)	0.0262(4)
C32	0.4114(2)	0.62209(19)	0.38320(13)	0.0366(5)
C34	0.47048(15)	0.41520(14)	0.14776(9)	0.0164(3)
C35	0.41314(15)	0.52533(14)	0.08664(9)	0.0173(3)

C36	0.29400(16)	0.55052(15)	0.05305(9)	0.0191(3)
C37	0.23679(16)	0.46539(15)	0.08154(10)	0.0191(3)
C38	0.29993(15)	0.35806(15)	0.14190(9)	0.0174(3)
C39	0.47884(16)	0.60893(15)	0.05965(10)	0.0201(3)
C40	0.53479(18)	0.67633(17)	0.03667(11)	0.0259(4)
P1	0.91753(4)	0.07849(4)	0.63543(3)	0.01945(9)
F1	0.77189(10)	0.10137(11)	0.61329(8)	0.0342(3)
F2	1.06165(11)	0.05864(13)	0.65717(9)	0.0424(3)
F3	0.92791(14)	-0.04413(12)	0.70349(9)	0.0504(4)
F4	0.97134(12)	0.00549(13)	0.57550(8)	0.0439(3)
F5	0.90455(13)	0.20274(12)	0.56596(8)	0.0429(3)
F6	0.86228(11)	0.15488(12)	0.69372(7)	0.0368(3)
P2	0.86742(4)	0.76441(4)	-0.00468(3)	0.02104(9)
F7	0.83036(18)	0.78269(12)	0.07795(8)	0.0564(4)
F8	0.89749(19)	0.75132(17)	-0.08864(9)	0.0644(5)
F9	0.71659(13)	0.81513(15)	-0.02793(10)	0.0695(6)
F10	0.86397(11)	0.90155(10)	-0.04003(7)	0.0306(2)
F11	1.01548(12)	0.71759(12)	0.01791(11)	0.0554(4)
F12	0.86992(12)	0.62856(11)	0.03176(8)	0.0373(3)
C41	0.8714(2)	0.33261(18)	0.77964(12)	0.0307(4)
C42	1.0085(2)	0.2875(3)	0.75661(19)	0.0539(7)
C43	0.8319(3)	0.2412(2)	0.84166(13)	0.0412(5)
O1	0.79828(19)	0.43755(14)	0.75071(11)	0.0501(4)
C44	0.7925(4)	0.4704(4)	0.2172(3)	0.0285(8)
C45	0.9341(4)	0.4331(4)	0.2064(3)	0.0467(10)
C46	0.7225(6)	0.5914(5)	0.2295(4)	0.0436(12)
O2	0.7350(3)	0.4074(3)	0.21545(17)	0.0437(6)
C47	0.7960(5)	0.5225(4)	0.2705(3)	0.0266(9)
C48	0.6794(7)	0.6370(7)	0.2342(5)	0.0403(16)
C49	0.8510(10)	0.4355(8)	0.2255(5)	0.052(2)
O3	0.8449(3)	0.5035(3)	0.33352(18)	0.0263(7)
C50	0.9372(4)	0.4879(4)	0.4842(3)	0.0275(9)
C51	0.8817(5)	0.4529(4)	0.5634(3)	0.0425(11)
C52	1.0506(5)	0.5301(5)	0.4789(3)	0.0392(11)
O4	0.8932(3)	0.4866(3)	0.42707(17)	0.0347(6)

$U_{eq}={}^{1}/_{3}[U_{11}(aa^*)^2+U_{22}(bb^*)^2+U_{33}(cc^*)^2+2U_{12}aa^*bb^*\cos\gamma+2U_{13}aa^*cc^*\cos\beta+2U_{23}bb^*cc^*\cos\alpha]$

Table S3. Positional Parameters for Hydrogens in [RuBEP]$(PF_6)_2$

Atom	x	y	z	U_{iso}, Å^2
H2	0.7632	0.2095	0.2178	0.025
H3	0.9235	0.1690	0.1319	0.029
H4	0.9089	0.0698	0.0473	0.031
H5	0.7349	0.0095	0.0542	0.029
H8	0.5881	-0.0732	0.0843	0.033
H9	0.4153	-0.1367	0.1141	0.036
H10	0.2665	-0.0653	0.2003	0.030
H11	0.2936	0.0662	0.2540	0.024
H14	0.7450	-0.0826	0.3117	0.026
H15	0.7882	-0.2811	0.3914	0.033
H16	0.6387	-0.3246	0.4816	0.035
H17	0.4508	-0.1651	0.4898	0.030
H20	0.2856	-0.0018	0.4957	0.027
H21	0.0982	0.1713	0.4815	0.031
H22	0.0766	0.3496	0.3775	0.032
H23	0.2386	0.3499	0.2911	0.026
H26	0.4265	0.3972	0.3097	0.023
H28	0.7113	0.3704	0.4441	0.028
H29	0.8329	0.1810	0.4302	0.026
H30	0.7473	0.1059	0.3580	0.023
H32	0.3608	0.6998	0.3846	0.049
H34	0.5502	0.3985	0.1700	0.022
H36	0.2535	0.6231	0.0122	0.025
H37	0.1569	0.4803	0.0603	0.025
H38	0.2613	0.3009	0.1600	0.023
H40	0.5786	0.7291	0.0187	0.034
H42a	1.0273	0.3552	0.7214	0.081
H42b	1.0201	0.2290	0.7310	0.081
H42c	1.0658	0.2495	0.8027	0.081
H43a	0.8614	0.2331	0.8922	0.062
H43b	0.8695	0.1636	0.8335	0.062
H43c	0.7394	0.2679	0.8392	0.062
H45a	0.9675	0.3548	0.1992	0.070
H45b	0.9768	0.4278	0.2521	0.070
H45c	0.9493	0.4926	0.1612	0.070
H46a	0.6326	0.6048	0.2359	0.065

H46b	0.7310	0.6558	0.1848	0.065
H46c	0.7591	0.5910	0.2757	0.065
H48a	0.6533	0.6840	0.2689	0.060
H48b	0.6099	0.6152	0.2253	0.060
H48c	0.7006	0.6847	0.1851	0.060
H49a	0.9247	0.3670	0.2547	0.077
H49b	0.8769	0.4766	0.1757	0.077
H49c	0.7866	0.4072	0.2171	0.077
H51a	0.8093	0.4324	0.5583	0.064
H51b	0.8537	0.5205	0.5827	0.064
H51c	0.9467	0.3836	0.5994	0.064
H52a	1.0786	0.5469	0.4262	0.059
H52b	1.1208	0.4668	0.5143	0.059
H52c	1.0229	0.6029	0.4928	0.059

Table S4. Refined Thermal Parameters (U's) for [RuBEP]$(PF_6)_2$

Atom	U_{11}	U_{22}	U_{33}	U_{23}	U_{13}	U_{12}
Ru1	0.01149(6)	0.01408(6)	0.01414(6)	-0.00525(4)	0.00267(4)	-0.00578(5)
N1	0.0133(6)	0.0157(6)	0.0157(6)	-0.0045(5)	0.0025(5)	-0.0053(5)
N12	0.0145(6)	0.0150(6)	0.0148(6)	-0.0042(5)	0.0016(5)	-0.0061(5)
N13	0.0141(6)	0.0169(6)	0.0169(6)	-0.0066(5)	0.0008(5)	-0.0066(5)
N24	0.0153(6)	0.0181(6)	0.0154(6)	-0.0072(5)	0.0027(5)	-0.0081(5)
N25	0.0160(6)	0.0164(6)	0.0146(6)	-0.0047(5)	0.0033(5)	-0.0075(5)
N33	0.0147(6)	0.0161(6)	0.0154(6)	-0.0066(5)	0.0031(5)	-0.0061(5)
C2	0.0170(7)	0.0220(8)	0.0192(7)	-0.0070(6)	0.0028(6)	-0.0095(6)
C3	0.0163(7)	0.0256(8)	0.0230(8)	-0.0052(7)	0.0047(6)	-0.0104(6)
C4	0.0195(8)	0.0262(8)	0.0232(8)	-0.0088(7)	0.0089(6)	-0.0080(7)
C5	0.0221(8)	0.0231(8)	0.0214(8)	-0.0104(7)	0.0061(6)	-0.0081(7)
C6	0.0153(7)	0.0157(7)	0.0182(7)	-0.0049(6)	0.0018(6)	-0.0052(6)
C7	0.0157(7)	0.0174(7)	0.0182(7)	-0.0063(6)	0.0017(6)	-0.0056(6)
C8	0.0229(8)	0.0274(9)	0.0298(9)	-0.0173(7)	0.0072(7)	-0.0103(7)
C9	0.0282(9)	0.0294(9)	0.0348(10)	-0.0196(8)	0.0052(7)	-0.0154(8)
C10	0.0225(8)	0.0247(8)	0.0258(8)	-0.0093(7)	0.0029(7)	-0.0140(7)
C11	0.0166(7)	0.0201(7)	0.0180(7)	-0.0060(6)	0.0025(6)	-0.0083(6)
C14	0.0156(7)	0.0212(8)	0.0218(8)	-0.0071(6)	0.0015(6)	-0.0071(6)
C15	0.0196(8)	0.0190(8)	0.0309(9)	-0.0071(7)	0.0000(7)	-0.0032(6)
C16	0.0274(9)	0.0174(8)	0.0291(9)	-0.0017(7)	-0.0009(7)	-0.0085(7)
C17	0.0221(8)	0.0221(8)	0.0225(8)	-0.0044(7)	0.0028(6)	-0.0113(7)
C18	0.0160(7)	0.0194(7)	0.0167(7)	-0.0068(6)	0.0013(6)	-0.0086(6)
C19	0.0172(7)	0.0184(7)	0.0159(7)	-0.0074(6)	0.0019(6)	-0.0090(6)
C20	0.0238(8)	0.0232(8)	0.0183(8)	-0.0077(6)	0.0056(6)	-0.0133(7)
C21	0.0216(8)	0.0295(9)	0.0246(8)	-0.0140(7)	0.0104(7)	-0.0126(7)
C22	0.0197(8)	0.0251(8)	0.0266(9)	-0.0131(7)	0.0069(7)	-0.0056(7)
C23	0.0189(8)	0.0198(8)	0.0201(8)	-0.0076(6)	0.0034(6)	-0.0064(6)
C26	0.0164(7)	0.0174(7)	0.0169(7)	-0.0052(6)	0.0029(6)	-0.0061(6)
C27	0.0222(8)	0.0189(8)	0.0203(8)	-0.0082(6)	0.0042(6)	-0.0083(6)
C28	0.0236(8)	0.0224(8)	0.0218(8)	-0.0097(6)	0.0009(6)	-0.0112(7)
C29	0.0173(7)	0.0211(8)	0.0202(8)	-0.0051(6)	-0.0007(6)	-0.0076(6)
C30	0.0162(7)	0.0167(7)	0.0178(7)	-0.0052(6)	0.0025(6)	-0.0062(6)
C31	0.0268(9)	0.0264(9)	0.0281(9)	-0.0135(7)	0.0001(7)	-0.0087(7)
C32	0.0350(11)	0.0292(10)	0.0446(12)	-0.0212(9)	-0.0036(9)	-0.0021(8)
C34	0.0151(7)	0.0194(7)	0.0174(7)	-0.0088(6)	0.0038(6)	-0.0075(6)
C35	0.0196(7)	0.0177(7)	0.0166(7)	-0.0082(6)	0.0067(6)	-0.0080(6)

C36	0.0200(8)	0.0171(7)	0.0172(7)	-0.0053(6)	0.0021(6)	-0.0042(6)
C37	0.0161(7)	0.0211(8)	0.0207(8)	-0.0088(6)	0.0009(6)	-0.0060(6)
C38	0.0153(7)	0.0188(7)	0.0210(8)	-0.0089(6)	0.0033(6)	-0.0082(6)
C39	0.0209(8)	0.0196(8)	0.0193(8)	-0.0077(6)	0.0049(6)	-0.0068(6)
C40	0.0298(9)	0.0251(9)	0.0268(9)	-0.0100(7)	0.0096(7)	-0.0149(7)
P1	0.01575(19)	0.0244(2)	0.0210(2)	-0.01088(17)	0.00422(15)	-0.00833(16)
F1	0.0199(5)	0.0419(7)	0.0526(7)	-0.0303(6)	0.0009(5)	-0.0113(5)
F2	0.0166(5)	0.0530(8)	0.0643(9)	-0.0304(7)	-0.0008(5)	-0.0103(5)
F3	0.0471(8)	0.0362(7)	0.0502(8)	0.0053(6)	0.0052(6)	-0.0149(6)
F4	0.0363(7)	0.0536(8)	0.0534(8)	-0.0411(7)	0.0134(6)	-0.0111(6)
F5	0.0426(7)	0.0355(7)	0.0405(7)	-0.0020(5)	0.0113(6)	-0.0151(6)
F6	0.0305(6)	0.0582(8)	0.0378(6)	-0.0358(6)	0.0084(5)	-0.0177(6)
P2	0.01733(19)	0.0287(2)	0.0218(2)	-0.01123(17)	0.00414(16)	-0.01182(17)
F7	0.1081(13)	0.0372(7)	0.0286(7)	-0.0170(6)	0.0303(7)	-0.0324(8)
F8	0.1137(14)	0.0909(12)	0.0411(8)	-0.0449(8)	0.0397(9)	-0.0807(12)
F9	0.0283(7)	0.0710(10)	0.0773(11)	0.0349(9)	-0.0177(7)	-0.0329(7)
F10	0.0297(6)	0.0302(6)	0.0310(6)	-0.0061(5)	0.0064(5)	-0.0148(5)
F11	0.0200(6)	0.0354(7)	0.0984(12)	-0.0064(7)	-0.0155(7)	-0.0078(5)
F12	0.0438(7)	0.0322(6)	0.0451(7)	-0.0163(5)	0.0065(6)	-0.0221(5)
C41	0.0405(11)	0.0273(9)	0.0309(10)	-0.0136(8)	-0.0054(8)	-0.0148(8)
C42	0.0437(13)	0.0595(16)	0.0807(19)	-0.0376(15)	0.0061(13)	-0.0310(12)
C43	0.0648(15)	0.0345(11)	0.0319(11)	-0.0191(9)	0.0104(10)	-0.0216(11)
O1	0.0649(12)	0.0273(8)	0.0487(10)	-0.0093(7)	-0.0069(8)	-0.0086(8)
C44	0.030(2)	0.035(2)	0.0234(18)	-0.0038(16)	0.0006(17)	-0.0205(18)
C45	0.033(2)	0.056(3)	0.047(2)	-0.0104(19)	-0.0049(18)	-0.0172(19)
C46	0.052(3)	0.039(3)	0.051(3)	-0.018(3)	0.016(3)	-0.029(3)
O2	0.0426(15)	0.0430(15)	0.0558(17)	-0.0174(13)	0.0019(12)	-0.0259(12)
C47	0.030(2)	0.024(2)	0.025(2)	0.0034(18)	0.0004(19)	-0.019(2)
C48	0.038(4)	0.042(4)	0.030(3)	0.003(3)	-0.011(3)	-0.013(3)
C49	0.062(6)	0.052(5)	0.042(4)	-0.021(4)	-0.008(5)	-0.018(4)
O3	0.0254(16)	0.0274(16)	0.0234(15)	-0.0020(13)	-0.0050(12)	-0.0114(13)
C50	0.0300(16)	0.0191(14)	0.0274(16)	-0.0095(14)	0.0036(14)	-0.0020(11)
C51	0.065(3)	0.041(2)	0.028(2)	-0.0137(18)	0.014(2)	-0.028(2)
C52	0.046(3)	0.032(2)	0.040(3)	-0.010(2)	-0.010(3)	-0.013(2)
O4	0.0321(15)	0.0307(14)	0.0386(16)	-0.0121(12)	0.0000(12)	-0.0082(12)

The form of the anisotropic displacement parameter is:

$\exp[-2\pi^2(a^{*2}U_{11}h^2+b^{*2}U_{22}k^2+c^{*2}U_{33}l^2+2b^*c^*U_{23}kl+2a^*c^*U_{13}hl+2a^*b^*U_{12}hk)]$

Table S5. Bond Distances in [RuBEP]$(PF_6)_2$, Å

Ru1-N13	2.0595(13)	Ru1-N12	2.0617(13)	Ru1-N24	2.0660(13)
Ru1-N1	2.0750(13)	Ru1-N33	2.0981(13)	Ru1-N25	2.1083(13)
N1-C2	1.345(2)	N1-C6	1.359(2)	N12-C11	1.344(2)
N12-C7	1.362(2)	N13-C14	1.345(2)	N13-C18	1.363(2)
N24-C23	1.345(2)	N24-C19	1.362(2)	N25-C26	1.349(2)
N25-C30	1.355(2)	N33-C34	1.346(2)	N33-C38	1.354(2)
C2-C3	1.384(2)	C3-C4	1.384(3)	C4-C5	1.388(2)
C5-C6	1.391(2)	C6-C7	1.476(2)	C7-C8	1.390(2)
C8-C9	1.384(2)	C9-C10	1.381(3)	C10-C11	1.382(2)
C14-C15	1.383(2)	C15-C16	1.387(3)	C16-C17	1.380(2)
C17-C18	1.392(2)	C18-C19	1.471(2)	C19-C20	1.388(2)
C20-C21	1.384(2)	C21-C22	1.384(3)	C22-C23	1.386(2)
C26-C27	1.398(2)	C27-C28	1.395(2)	C27-C31	1.438(2)
C28-C29	1.386(2)	C29-C30	1.383(2)	C31-C32	1.182(3)
C34-C35	1.397(2)	C35-C36	1.391(2)	C35-C39	1.439(2)
C36-C37	1.385(2)	C37-C38	1.383(2)	C39-C40	1.187(3)
P1-F3	1.5831(13)	P1-F4	1.5904(12)	P1-F6	1.5956(11)
P1-F2	1.5998(12)	P1-F5	1.6021(13)	P1-F1	1.6064(11)
P2-F11	1.5717(13)	P2-F8	1.5821(14)	P2-F7	1.5907(13)
P2-F12	1.5967(12)	P2-F9	1.5980(13)	P2-F10	1.6070(12)
C41-O1	1.207(3)	C41-C43	1.488(3)	C41-C42	1.498(3)
C44-O2	1.205(4)	C44-C45	1.490(5)	C44-C46	1.504(6)
C47-O3	1.217(5)	C47-C49	1.499(7)	C47-C48	1.506(6)
C50-O4	1.192(5)	C50-C51	1.509(5)	C50-C52	1.538(6)

Table S6. Bond Angles in [RuBEP]$(PF_6)_2$, °

N13-Ru1-N12	83.17(5)	N13-Ru1-N24	78.73(5)	N12-Ru1-N24	96.51(5)
N13-Ru1-N1	97.01(5)	N12-Ru1-N1	78.84(5)	N24-Ru1-N1	174.11(5)
N13-Ru1-N33	172.47(5)	N12-Ru1-N33	91.25(5)	N24-Ru1-N33	96.99(5)
N1-Ru1-N33	86.80(5)	N13-Ru1-N25	93.45(5)	N12-Ru1-N25	174.24(5)
N24-Ru1-N25	87.36(5)	N1-Ru1-N25	97.01(5)	N33-Ru1-N25	92.52(5)
C2-N1-C6	118.06(13)	C2-N1-Ru1	126.69(11)	C6-N1-Ru1	115.21(10)
C11-N12-C7	118.18(14)	C11-N12-Ru1	125.44(11)	C7-N12-Ru1	115.65(10)
C14-N13-C18	118.04(14)	C14-N13-Ru1	125.13(11)	C18-N13-Ru1	115.42(10)
C23-N24-C19	117.88(13)	C23-N24-Ru1	126.67(11)	C19-N24-Ru1	115.45(10)
C26-N25-C30	117.15(14)	C26-N25-Ru1	123.00(11)	C30-N25-Ru1	119.83(10)
C34-N33-C38	117.45(14)	C34-N33-Ru1	122.42(11)	C38-N33-Ru1	120.04(10)
N1-C2-C3	123.04(15)	C2-C3-C4	118.81(15)	C3-C4-C5	119.01(15)
C4-C5-C6	119.28(16)	N1-C6-C5	121.77(15)	N1-C6-C7	115.09(14)
C5-C6-C7	123.14(15)	N12-C7-C8	121.53(15)	N12-C7-C6	114.77(14)
C8-C7-C6	123.64(15)	C9-C8-C7	119.35(16)	C10-C9-C8	119.12(16)
C9-C10-C11	118.91(16)	N12-C11-C10	122.89(15)	N13-C14-C15	122.82(15)
C14-C15-C16	119.12(16)	C17-C16-C15	118.79(16)	C16-C17-C18	119.60(16)
N13-C18-C17	121.61(15)	N13-C18-C19	114.62(14)	C17-C18-C19	123.71(14)
N24-C19-C20	121.75(15)	N24-C19-C18	114.87(13)	C20-C19-C18	123.38(15)
C21-C20-C19	119.82(16)	C22-C21-C20	118.42(15)	C21-C22-C23	119.33(16)
N24-C23-C22	122.79(16)	N25-C26-C27	123.01(15)	C28-C27-C26	118.87(15)
C28-C27-C31	121.66(16)	C26-C27-C31	119.46(15)	C29-C28-C27	118.30(15)
C30-C29-C28	119.51(15)	N25-C30-C29	123.16(15)	C32-C31-C27	178.6(2)
N33-C34-C35	122.86(15)	C36-C35-C34	118.75(15)	C36-C35-C39	121.81(15)
C34-C35-C39	119.44(15)	C37-C36-C35	118.71(15)	C38-C37-C36	119.18(15)
N33-C38-C37	123.05(15)	C40-C39-C35	178.65(18)	F3-P1-F4	90.54(8)
F3-P1-F6	90.85(8)	F4-P1-F6	178.55(8)	F3-P1-F2	91.13(8)
F4-P1-F2	90.12(7)	F6-P1-F2	90.26(7)	F3-P1-F5	178.94(8)
F4-P1-F5	89.28(8)	F6-P1-F5	89.32(7)	F2-P1-F5	89.91(8)
F3-P1-F1	89.77(8)	F4-P1-F1	90.64(7)	F6-P1-F1	88.97(6)
F2-P1-F1	178.82(7)	F5-P1-F1	89.19(7)	F11-P2-F8	91.44(10)
F11-P2-F7	91.11(10)	F8-P2-F7	177.15(11)	F11-P2-F12	91.15(7)
F8-P2-F12	91.85(8)	F7-P2-F12	89.35(7)	F11-P2-F9	178.68(9)
F8-P2-F9	88.88(11)	F7-P2-F9	88.54(10)	F12-P2-F9	90.12(8)

F11-P2-F10	88.99(7)	F8-P2-F10	89.09(7)	F7-P2-F10	89.69(7)
F12-P2-F10	179.04(7)	F9-P2-F10	89.74(7)	O1-C41-C43	122.0(2)
O1-C41-C42	121.9(2)	C43-C41-C42	116.0(2)	O2-C44-C45	121.9(4)
O2-C44-C46	120.7(4)	C45-C44-C46	117.4(4)	O3-C47-C49	121.7(5)
O3-C47-C48	120.6(5)	C49-C47-C48	117.7(5)	O4-C50-C51	121.7(4)
O4-C50-C52	120.6(5)	C51-C50-C52	117.7(5)		

Figure S3. Electrospray mass spectrometry of [RuBEP]$(PF_6)_2$+/- light

Sample was prepared in 50% acetonitrile 0.1% formic acid stock solution, and directly infused as nanospray onto a Thermo ORBI trap XL mass spectrometer at 60 K resolution.

Before irradiation - expected mass = 620.13 Da

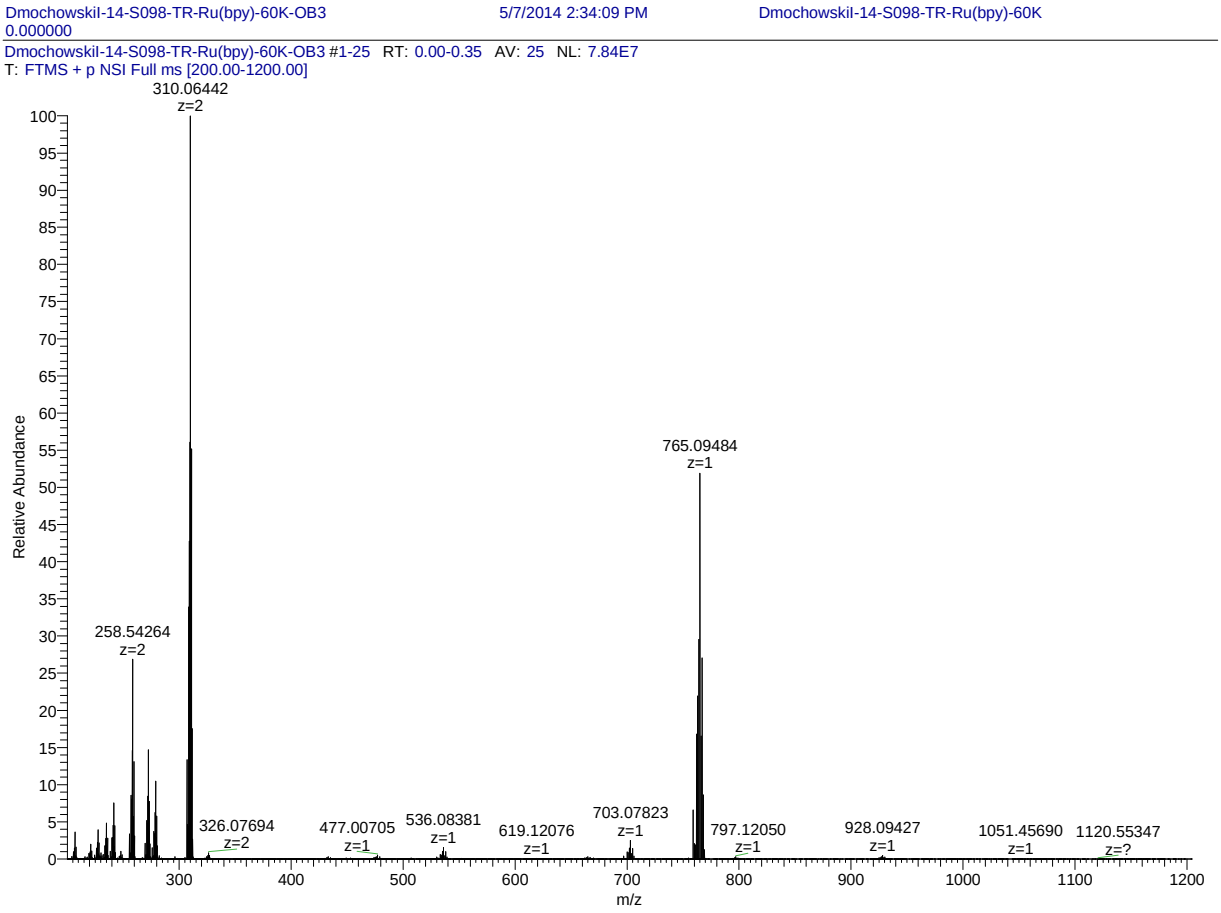

Compound	Expected Mass (Da)	Observed Mass (Da)
Ru(bipyridine)$_2$(3-ethynylpyridine)$_2^{+2}$	310.06*	310.1
Ru(bipyridine)$_2$(3-ethynylpyridine)$_2$[PF_6]	764.6	765.1

*Doubly charged peak

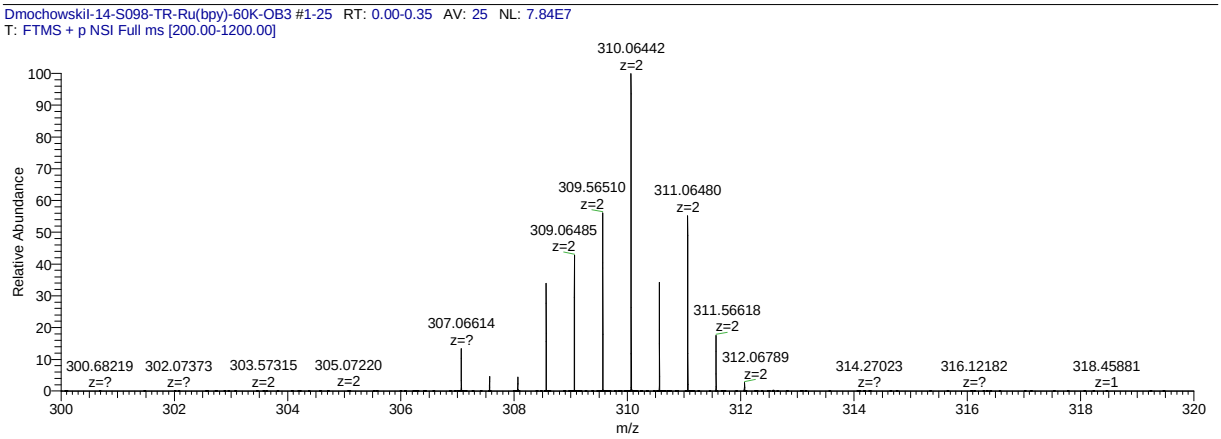

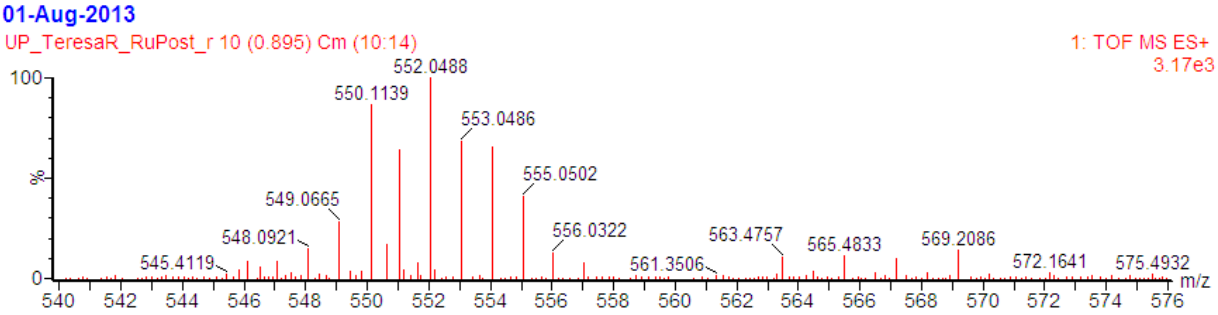

Hi-Res MS after irradiation at 450 nm (3 min, 14 mW/cm^2)

After irradiation: Expected mass = 552.02 Da for [Ru(bpy)$_2$(3EP)OH]

Figure S4. ^{1}H NMR, pre- and post-photolysis of RuBEP in D_2O.

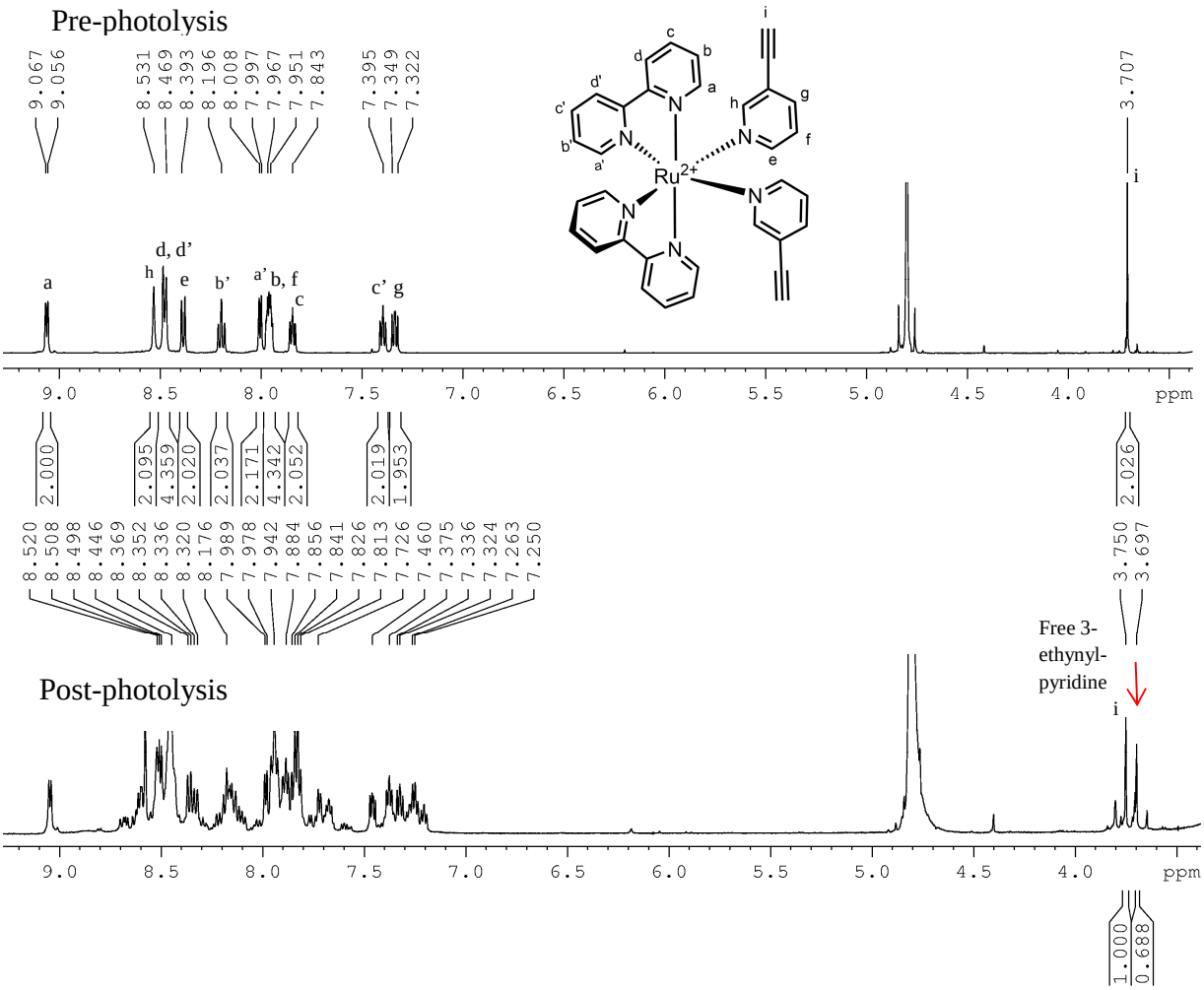

The appearance of a second major peak in the alkyne region shows that one ligand exchanged with solvent (D_2O), and one remained coordinated to ruthenium. The loss of symmetry in the remaining complex gives a more complex peak pattern in the aromatic region.

Figure S5. Kinetics trace of photolysis reaction

Light source: 450 nm laser (14 mW/cm^2), 14 μM RuBEP in water, 0.2 OD. Quantum yield of photorelease = 0.33 ± 0.06.

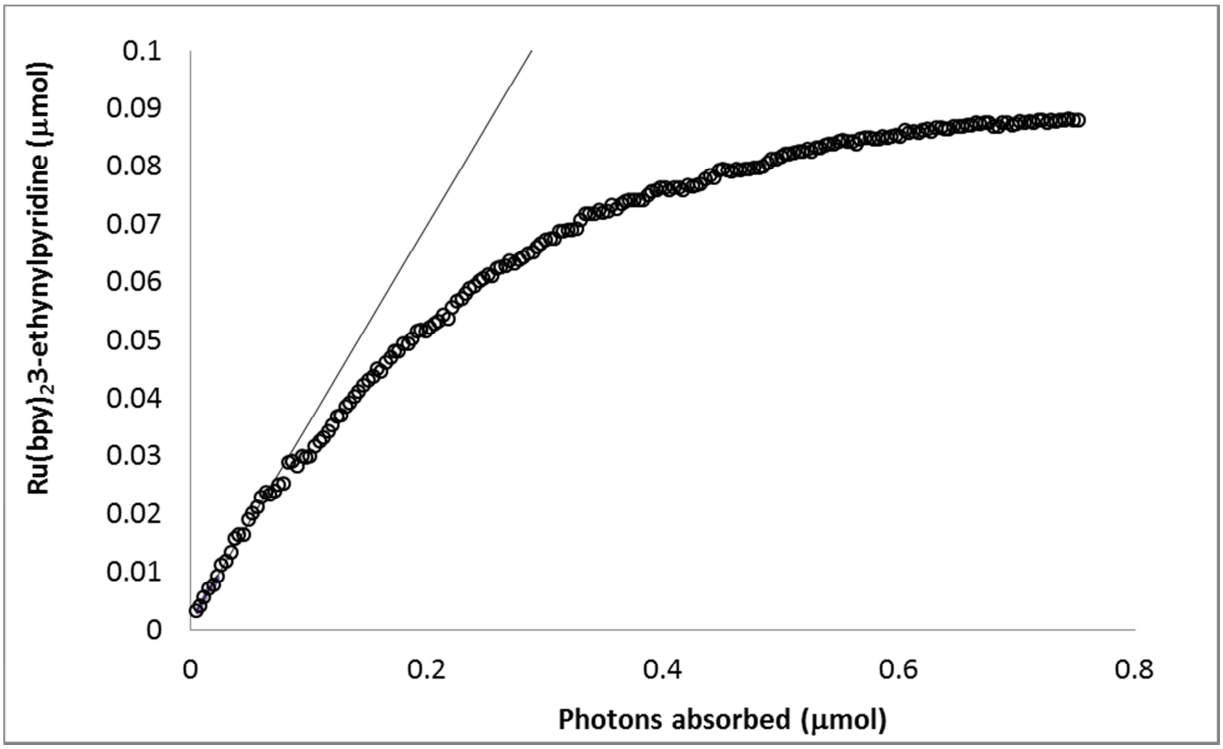

Moles Product $Ru(bpy)_2 3EP(OH_2)$ = initial moles RuBEP – current moles RuBEP (1)

$$\text{current moles RuBEP} = \left(\frac{\text{Abs}-\varepsilon_p[\text{RuBEP}]_i}{\varepsilon_s-\varepsilon_p}\right)\times V_{cuvet} \quad (2)$$

$$\text{photons absorbed} = \frac{E}{P_l} \quad (3)$$

Where:
P_l = net power of the laser during the trial (mW)
E = energy of 450 nm light (J/photon)
ε_s = extinction coefficient of RuBEP (starting material) at 475 nm = 1800 $M^{-1}cm^{-1}$
ε_p = extinction coefficient of $Rubpy_2(3EP)(H_2O)$ (product) at 475 nm = 3800 $M^{-1}cm^{-1}$

Methods S2. Circularization procedure for DNA and morpholino

Ru-oligo cyclization reactions were performed on a 10-12 nmol scale. Mono-azido DNA and bis-azido DNA were purchased from Integrated DNA Technologies, Coralville, Iowa. Bis-azido morpholinos were custom ordered from GeneTools, Philomath, Oregon. Bis-azido oligonucleotides were premixed with RuBEP at the indicated stoichiometric ratios in water. CuBr was dissolved in 3:1 DMSO/t-butanol to make a 0.1 M solution. TBTA ([(1-benzyl-1*H*-1,2,3-triazol-4-yl)methyl]amine) (Anaspec, Freemont, CA) was dissolved in 3:1 DMSO/t-butanol to make a 0.1 M solution. CuBr and TBTA were mixed in a 1:2 ratio and preincubated. The azide/alkyne solution volume was adjusted to 25 µL (0.4 mM) (for morpholino reactions) and 50 µL (0.2 mM) (for DNA reactions). 12 vol% of the premixed CuBr/TBTA solution was added to the oligonucleotide solution. Solutions were sparged with N_2 and sealed tightly with parafilm. Reactions proceeded for 3 h (DNA) and 18-48 h (MO). Temperatures varying from RT to 55 °C were tested, and no significant correlation was found between temperature and product formation. Additionally, vortexing or not mixing did not seem to change product formation. After reaction completion, a NAP-5 desalting column (GE Healthcare) was used to remove unreacted RuBEP, CuBr, and TBTA. Circular product was stored in molecular biology grade water at -20 °C.

Reagent	**nmol**
Bis-azido-oligo	10 - 12
RuBEP	10.
CuBr	100.
TBTA	200.

Figure S6. Time-course gel of DNA circularization

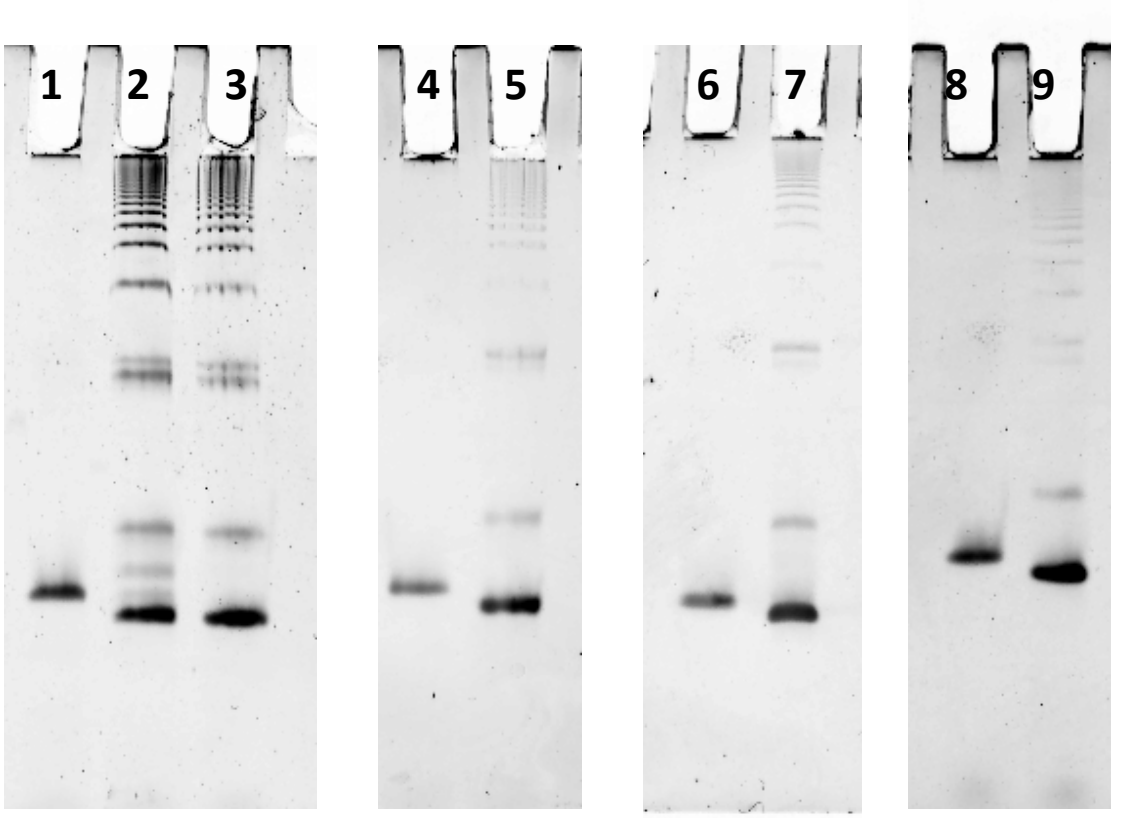

25 pmol aliquots were removed over the course of the DNA circularization reaction. Each aliquot was run on a 15% PAGE/ 7M urea gel at 300 V for 45 min and stained for 15 min with EtBr. Click reaction aliquots were compared to the linear bis-azido DNA migration (lanes 1, 4, 6, 8). Circular product appeared as the fastest migrating band, within the first 15 min of the reaction, with more product formation at 3 h (lane 9).

Figure S7. Mono-azide DNA click reaction

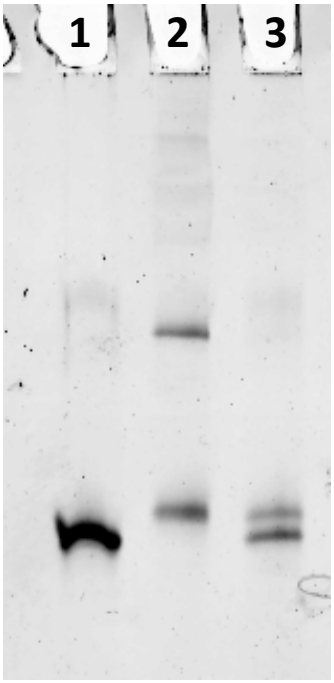

1 – N_3-DNA only
2 – N_3-DNA clicked
3 – N_3-DNA clicked
+ 450 nm light (3 min)

A mono-azido DNA 25mer was subjected to the same conditions given above for the bis-azide DNA. The reaction efficiency was monitored on a 15% PAGE/7 M urea gel, run for 45 min at 300 V. The gel was stained for 15 min with EtBr. A band (lane 2) corresponding to linear Ru-DNA ran slightly slower than the N_3-DNA (lane 1), and its intensity decreased after photolysis (lane 3). Only 50% decrease in photolysis was seen, as only one 3EP ligand on RuBEP exchanged upon light exposure and roughly half of the DNA remained Ru-bound. The much slower moving band in lane 2 was likely DNA-RuBEP-DNA.

Figure S8. HPLC procedure and traces for N_3-DNA, linear Ru-DNA, N_3-DNA-N_3, and circular Ru-DNA

A gradient of increasing acetonitrile in 0.05 M triethylammonium acetate in H_2O was used with a Zorbax reverse-phase C18 column. The column was heated to 40 °C during purification. Product elution times are indicated on HPLC traces.

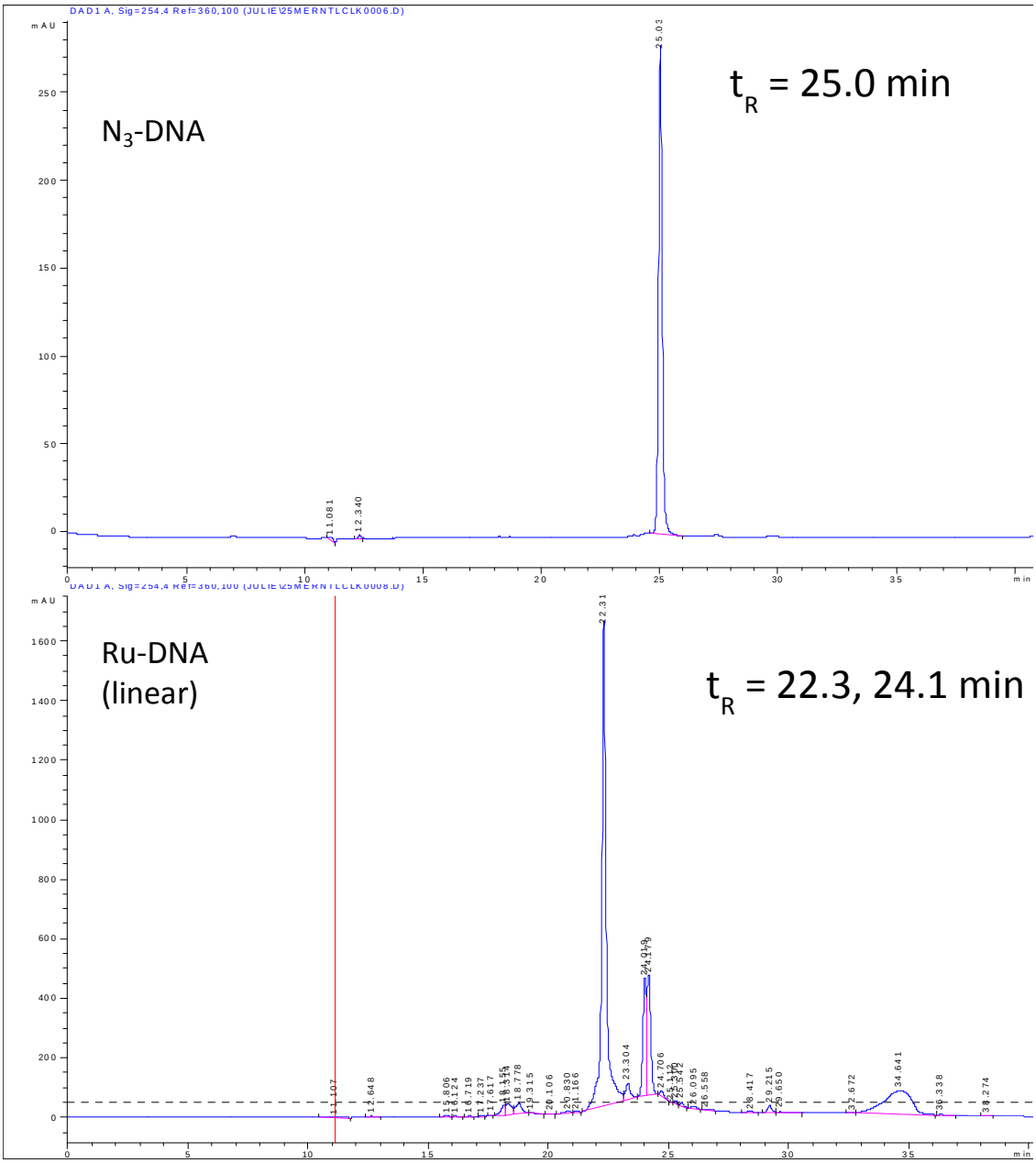

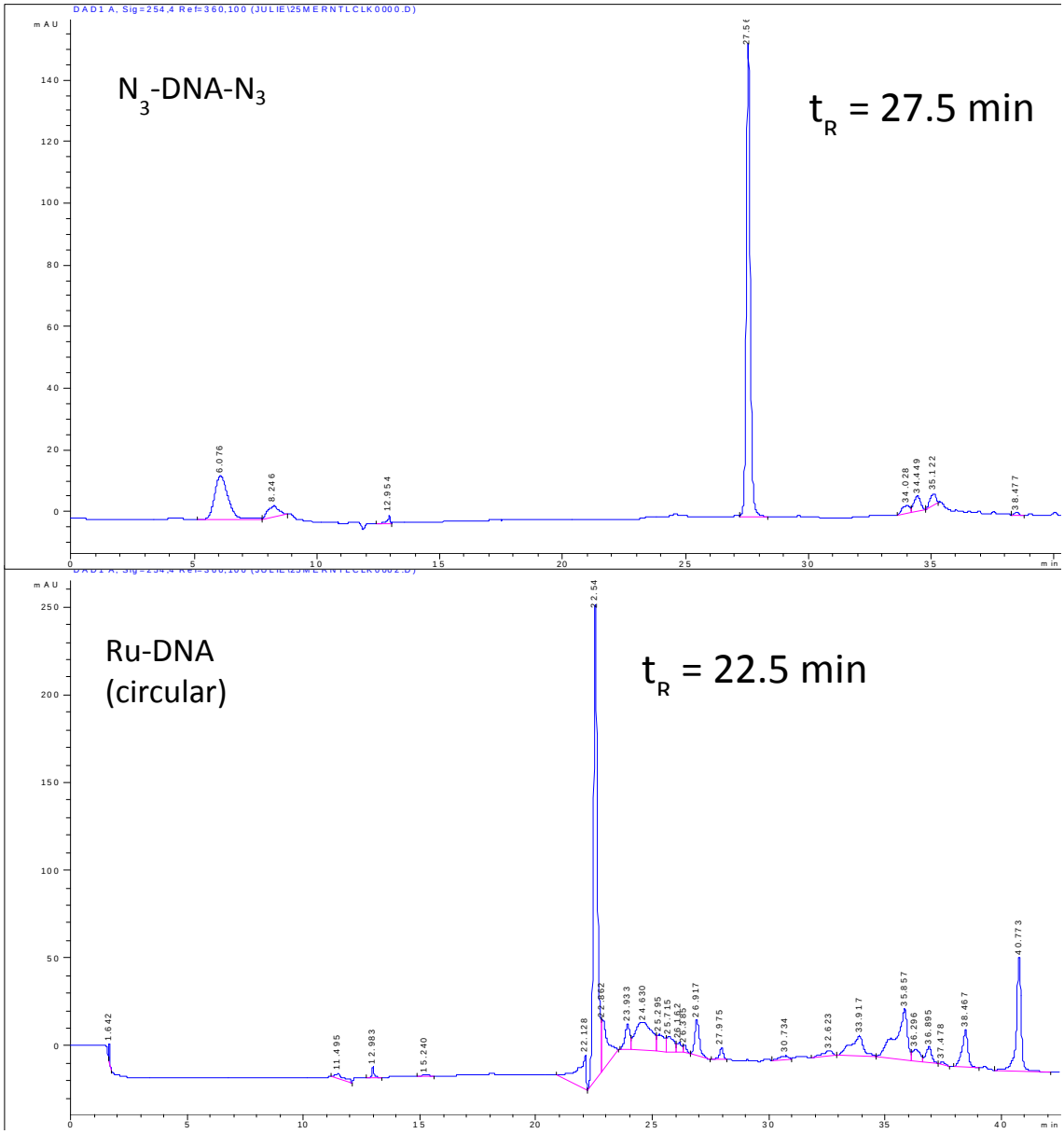
DAD1 A, Sig=254,4 Ref=360,100 (JULIE\25MERNTLCLK0000.D)
mAU
N_3-DNA-N_3
t_R = 27.5 min
6.076
8.246
12.954
27.551
34.028
34.449
35.122
38.477
min
Ru-DNA
(circular)
t_R = 22.5 min
1.642
11.495
12.983
15.240
22.128
22.540
23.933
24.630
25.295
25.715
26.062
26.385
26.917
27.975
30.734
32.623
33.917
35.857
36.295
36.895
37.478
38.467
40.773

Table S7. Gradient used for linear Ru-DNA and circular Ru-DNA HPLC purification

Time (min)	% Acetonitrile	% 0.05 M TEAA
0.0	90	10
40.0	40	60
50.0	20	80

Figure S9. 20%, 7 M urea PAGE analysis of Ru-DNA after HPLC purification and irradiation

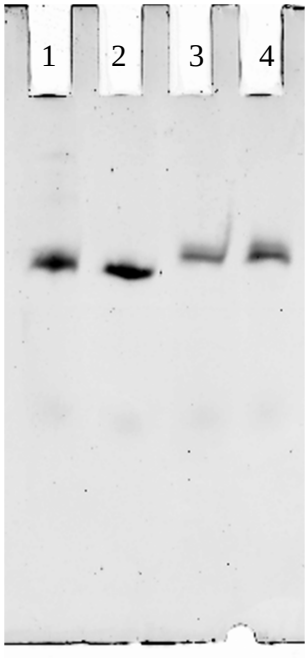

1) Linear DNA (T_R = 27.5 min)
2) Ru-DNA after HPLC purification (T_R = 22.5 min)
3) Ru-DNA + 450 nm light (3 min)
4) Ru-DNA + 450 nm light, after 24 h

Gel (lane 4) shows no recombination after 24 h sitting at room temperature (21 °C). The band corresponding to uncaged, linear DNA (lane 3) shows no difference between immediate irradiation and 24 h post-irradiation (lane 4).

Denaturing gel: 15% PAGE/7M urea, 300 V, 45 min.

Figure S10. MALDI-TOF MS data for Ru-DNA

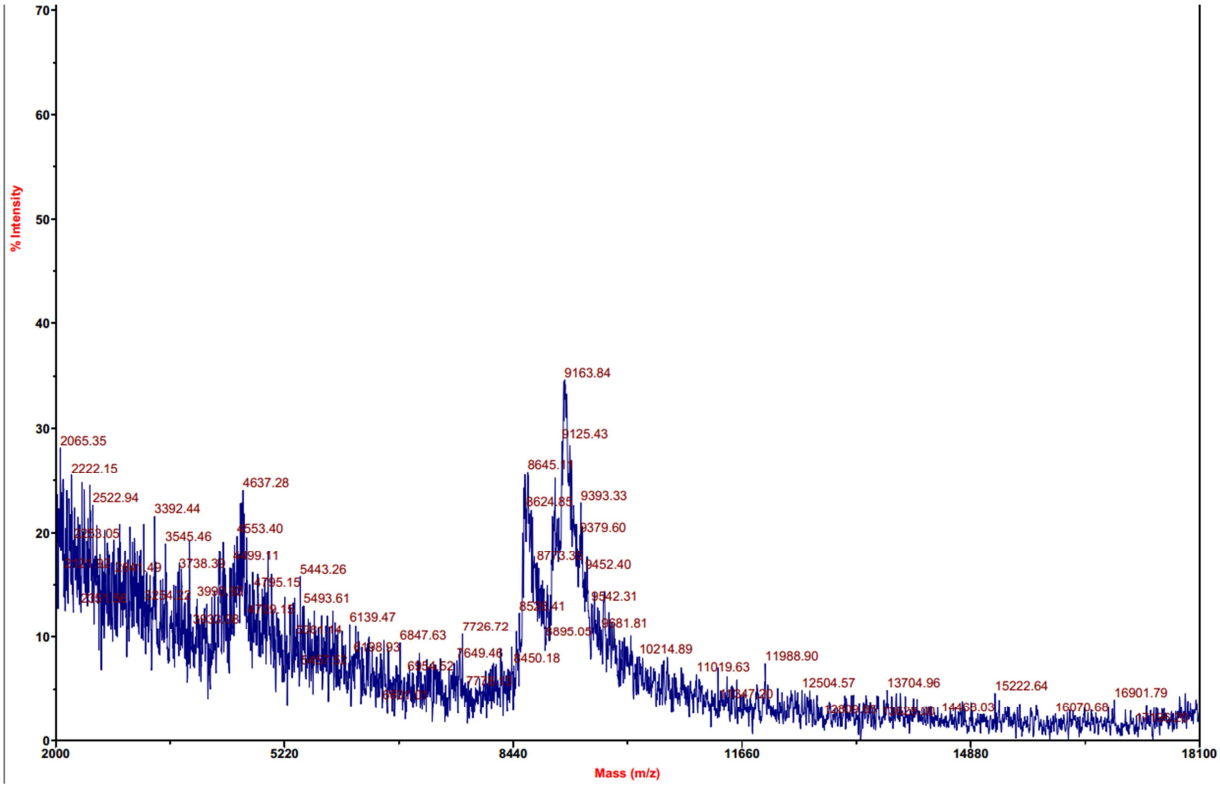

	Expected Mass (Da)	Observed Mass (Da)
Ru-DNA[Cl][PF_6]	9166	9163
Ru-DNA[PF_6][Cl] w/o $Ru(bpy)_2$	8642	8645

Table S8. MALDI-MS data

	Expected mass (Da)	**MALDI mass (Da)**
Ru-DNA*	9166	9163
Ru-MO-*chd*	9561	9567
Ru-MO-*ntl*	9357	9385

Ru-MO samples were analyzed using 3-hydroxypicolinic acid (3-HPA) matrix in linear positive ion mode on a Bruker Ultraflex III MALDI-TOF/TOF mass spectrometer.

*Ru-DNA[PF_6][Cl]: MALDI was performed by the Wistar Proteomics Facility at the University of Pennsylvania. All masses were attained in linear negative mode on an Applied Biosystems Voyager-DE® PRO MALDI TOF Mass Spectrometer, using 3-hydroxypicolinic acid (3-HPA) matrix.

Method S3. Molecular beacon hybridization assay

Molecular beacons (Integrated DNA Technologies, Coralville, IA), complementary to the zebrafish *chd* and *ntl* MO sequence was designed, with fluorophore, 6-FAM on the 5′ end and quencher, BHQ1 on the 3′ end. Caging, indicative of circularization, was monitored by the opening of the molecular beacon in the presence of oligonucleotide.

A 3-fold excess of target sample (mismatched sequence, linear DNA or MO, Ru-MO/Ru-DNA, or its post-irradiation counterpart) was combined (mixed and gently vortexed) with the molecular beacon and allowed to hybridize over 20 min at 25 °C to best approximate physiological conditions. Irradiated samples were photolysed (3 min, 450 nm, 14 mW/cm^2) prior to addition of the beacon. The fluorescence intensity was then measured (λ_{ex} = 454 nm, λ_{em} = 513 nm). Significant decrease in fluorescence for the circularized Ru-MO/Ru-DNA sample relative to the linear MO indicated caging.

The beacon used for the Ru-MO had a higher melting point of activation than the beacon employed for Ru-DNA, which decreased the maximum fluorescence intensity observed. As such, the difference between the maximum and the minimum fluorescence intensity observed (for both the mismatched sequence and the caged Ru-MO) was less than that observed for the Ru-DNA molecular beacon reported in this work.

All solutions contained 1 pmol/μL of molecular beacon in a total volume of 70 μL.

Methods S4. Zebrafish microinjection experimental details

Zebrafish embryos were obtained from the CDB Zebrafish Core Facility at the University of Pennsylvania Perelman School of Medicine. All embryos obtained were TLF x TLF WT. Zebrafish embryo injection solutions were prepared to contain a final concentration of 0.1 M KCl and 0.25% phenol red dye. All injections were performed at the one-cell stage and injected into the cell compartment only. A Harvard Apparatus PLI-100 pico-injector was used to inject controlled volumes. Injection volume was calibrated to dispense 5 nL per embryo. Zebrafish embryos were incubated at 28 °C in E3 zebrafish medium. All embryos were incubated in the dark, except for irradiated embryos, which were exposed to 450-nm light (14 mW/cm^2, 5 min) at 1 hpf and returned to the dark incubator. Embryo micrographs were collected at 24 hpf with an Olympus FV1000 laser scanning confocal microscope using transmitted light imaging. A 10x air objective was used for single embryo imaging.

Figure S11. *chd*-MO knockdown phenotype

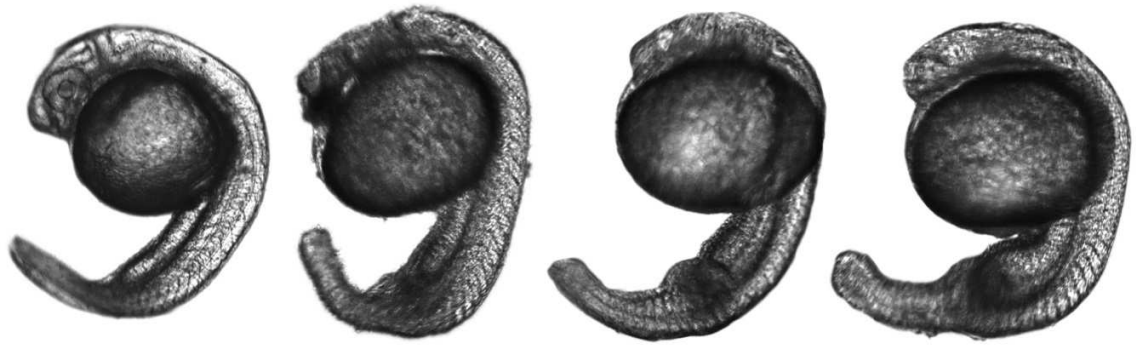

Normal WT **Mild** **Moderate** **Severe**

Zebrafish embryos were injected at the 1-cell stage with 0.51 mM *chd*-MO and imaged at 24 hpf. The *chordin* morpholino knockdown phenotype ranged from severe to mild. Embryos scored as normal had V-shaped somites, and normal head and tail development. Severe was identified by decreased head size, U-shaped somites, and a large blood island on the tail. The moderate and mild phenotypes were identified by U-shaped somites and a medium or small blood island on the tail.

Figure S12. *ntl*-MO circularization

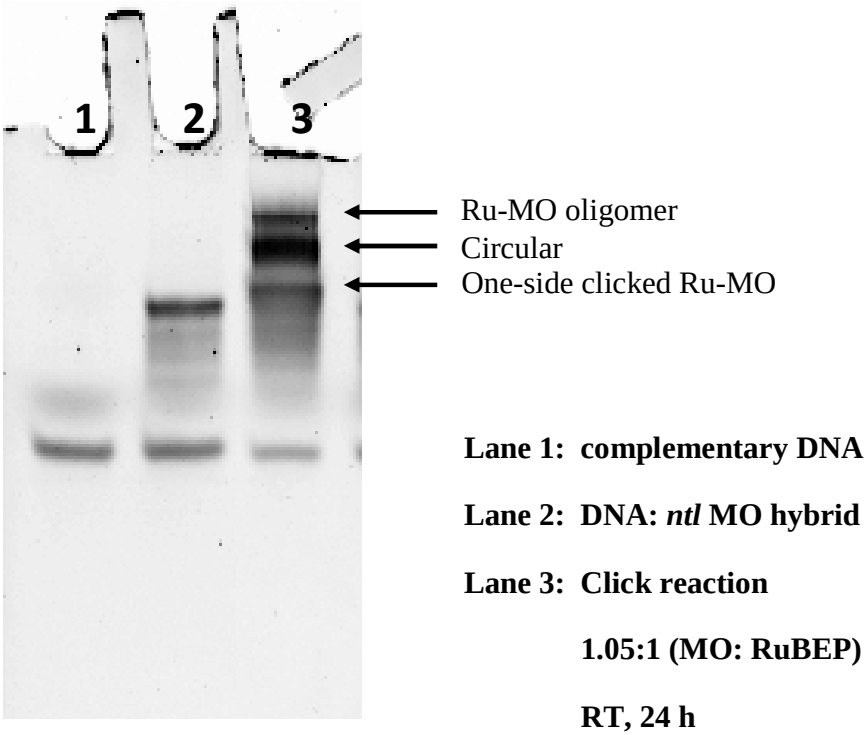

15% native PAGE gel-shift assay showing controls (lanes 1 and 2) and formation of Ru-MO-*ntl* (lane 3). No additional purification was performed before *in vivo* testing. Due to initial impurities of bis-azido-*ntl* MO, the same circularization efficiency could not be achieved as with bis-azido-*chd* MO.

Figure S13. *ntl*-MO knockdown phenotype

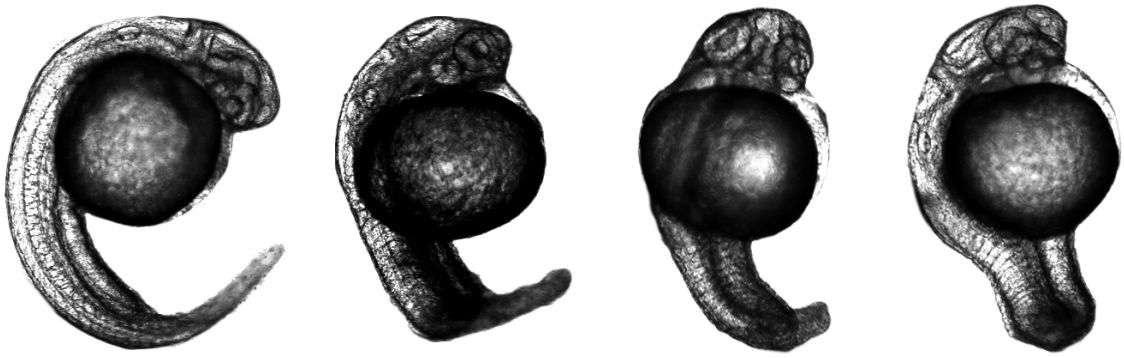

Normal WT (Class 1) **Class 2** **Class 3** **Class 4**

Zebrafish embryos were injected at the 1-cell stage with 0.25 mM *ntl*-MO and imaged at 24 hpf. The *notail* morpholino knockdown phenotype ranged from severe (class 4) to mild (class 2) where severe was identified by a significantly decreased head size, U-shaped somites, no notochord, and no posterior structures. Class 3 was identified by U-shaped somites, no notochord, and significantly shortened posterior structures. Class 2 was identified by U-shaped somites, a shortened posterior axis, with the notochord still present.

Figure S14. Ru-MO-*ntl in vivo* data

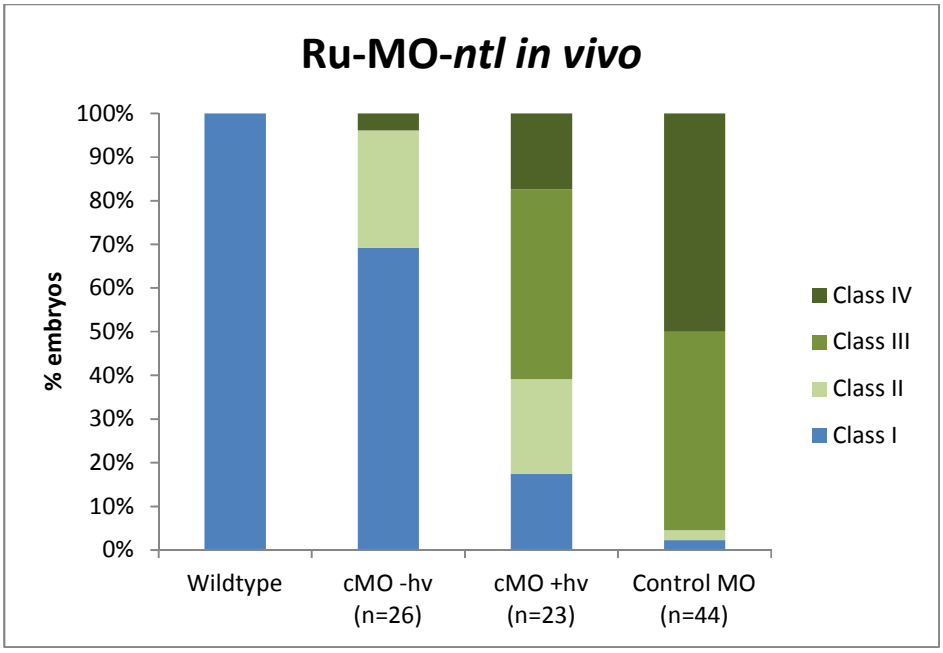

MO Control: Zebrafish embryos were injected at the 1-cell stage with 0.25 mM *ntl*-MO and imaged at 24 hpf.

Ru-MO-*ntl:* Zebrafish embryos were injected at the 1-cell stage with 0.25 mM Ru-MO-*ntl*. Half of the embryos were irradiated (450 nm, 14 mW/cm^2, 5 min) at 1 hpf, while the other half were incubated in the dark. Embryos were scored for phenotype at 24 hpf and compared to wildtype.

Decreased uncaging efficiency of the caged Ru-MO-*ntl* is attributed to decreased purity of the injected Ru-MO.

Figure S15. RuBEP +/- light *in vivo* control

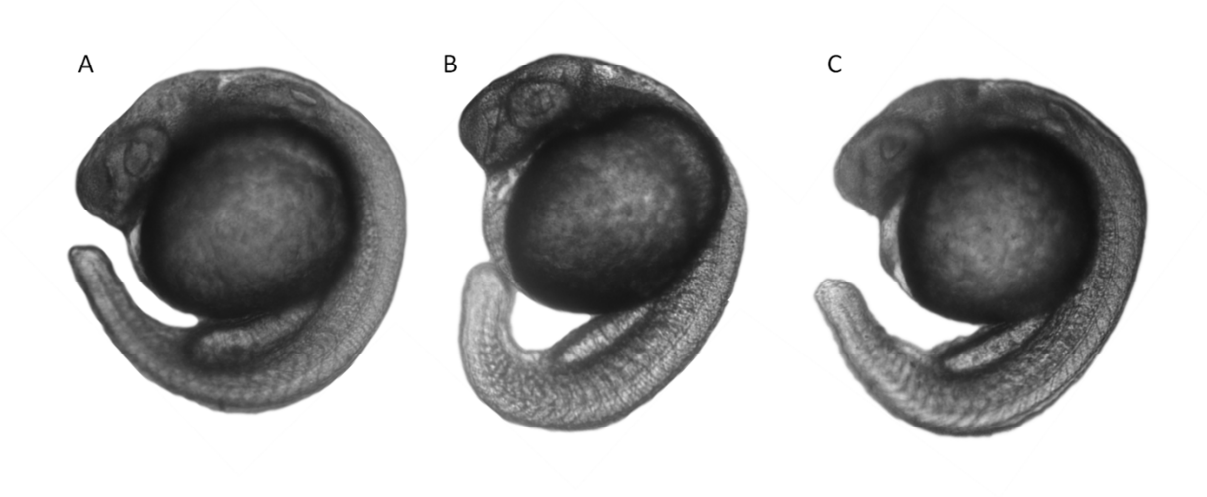

A) Uninjected wildtype zebrafish embryo. B) Zebrafish embryo injected at the 1-cell stage with 500 µM RuBEP and incubated in the dark. C) Zebrafish embryo injected at the 1-cell stage with 500 µM RuBEP and irradiated (450 nm, 14 mW/cm^2, 15 min). All embryos showed normal development (n > 50).

Figure S16. Scramble morpholino *in vivo* control

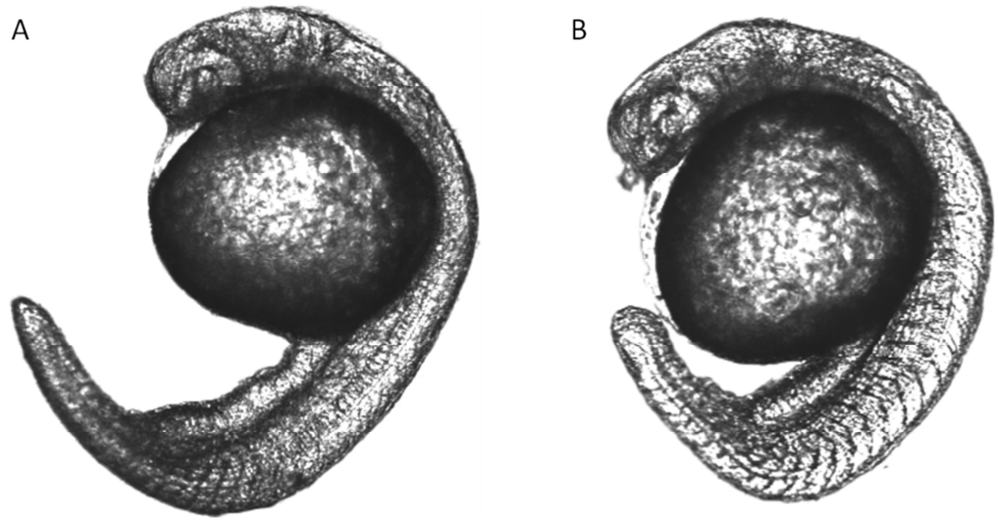

A) Uninjected wildtype zebrafish embryo. B) Zebrafish embryo injected at the 1-cell stage with 500 µM standard scramble control morpholino (see sequence, Table S9). All embryos showed normal development (n > 50).

Table S9. Oligonucleotide sequences, 5′ to 3′

DNA	GACTTGAGGCAGGCATATTTCCGAT
reverse complement	ATCGGAAATATGCCTGCCTCAAGTC
molecular beacon	6FAM- CCACCCATCGGAAATATGCCTGCCTCAAGTCGGGTGG- BHQ1
***chd*-MO**	ATCCACAGCAGCCCCTCCATCATCC
***chd* reverse complement**	GGATGATGGAGGGGCTGCTGTGGAT
***chd* molecular beacon**	6FAM- CGGGC GGGATGATGGAGGGGCTGCTGTGGATCGCCCG- BHQ1
ntl* MO	AGCTTGAGATAAGTCCGACGATCCT
***ntl* reverse complement**	AGGATCGTCGGACTTATCTCAAGCT
standard control MO	CCTCTTACCTCAGTTACAATTTATA

***notail* MO sequence used was *nt2*-MO from Tallafuss et. al.[1]**

Methods S5. Instrumentation

A Luxeon III Star® Royal Blue© LED was used for uncaging experiments post-click reactions, including *in vivo* work. It was purchased from Quadica Developments Inc. (Ontario, Canada) with a maximum output wavelength of 450 nm. Measured power at sample was 14 mW/cm^2.

A sapphire Galaxy Blue handheld laser was purchased from Beam of Light Technologies (Oregon, USA) and used to determine the quantum yield of RuBEP. Measured power at the sample was 53 mW/cm^2, with a maximum output wavelength of 450 nm.

UV-Vis spectroscopy was performed using an Agilent 8453 UV-Vis spectrometer (Agilent Technologies, Germany) in water unless otherwise specified. ^1H NMR spectra were obtained on a Bruker DMX 500 spectrometer, and ^{13}C NMR spectra were obtained using a Bruker AVIII cryo500 probe spectrometer at the University of Pennsylvania NMR facility and were recorded at room temperature. The ^1H and ^{13}C spectra were referenced to the central line of the solvent residual or to TMS at 0.00 ppm. ^1H NMR and ^{13}C NMR chemical shifts (δ) are given in parts per million and reported to a precision of ± 0.01 and ± 0.1 ppm, respectively. Proton coupling constants (J) are given in Hz and reported to a precision of ± 0.1 Hz.

High-resolution mass spectra (HRMS) were obtained using electrospray ionization (ESI) mass spectrometry on a Micromass Autospec at the Mass Spectrometry Facility in the Department of Chemistry at the University of Pennsylvania. Irradiated sample was analyzed via direct infusion nanospray with a Thermo ORBI trap XL mass spectrometer at 60 K resolution. Gels were imaged with a Typhoon FLA 7000 imaging system (GE Healthcare Life Sciences, Pittsburgh, PA).

All oligo purifications were performed with Agilent 1200 Analytical HPLC using a diode-array detector set to 260 nm. A 5-micron Zorbax semi-preparatory C18 column (9.4 x 215 mm) was used for all reverse-phase purifications.

Methods S6. Materials

Organic reagents and solvents were used as purchased from the following chemical sources:

Fisher: methanol, methylene chloride (HPLC grade), acetonitrile (HPLC grade), acetone.

Acros Organics: cis-dichloro-bis(2,2′-bipyridine)ruthenium(II) (98%), 3-ethynylpyridine (96%), silver trifluoromethansulfonate (99+%), ammonium hexafluorophosphate (99.5%), acetonitrile-d^3 (99.8 atom%), tetrabutylammonium chloride hydrate (98%), deuterium oxide (99.8 atom%)

Complementary DNA oligonucleotides, azido-DNA oligonucleotides, and molecular beacons were custom synthesized and HPLC purified by Integrated DNA technologies (Coralville, IA). Azido-MOs were custom synthesized by Gene Tools (Philomath, Oregon). All gel reagents were purchased from Bio-Rad (Hercules, CA). TBTA ligand (Tris[(1-benzyl-1*H*-1,2,3-triazol-4-yl)methyl]amine) was purchased through Anaspec (Fremont, CA). Zebrafish embryos were obtained through the CDB Zebrafish Core Facility at the University of Pennsylvania Perelman School of Medicine.

Reference

(1) Tallafuss, A.; Gibson, D.; Morcos, P.; Li, Y.; Seredick, S.; Eisen, J.; Washbourne, P. *Development (Cambridge, England)* **2012**, *139*, 1691-1699.